Highly Maneuverable Aircraft Technology (HiMAT) Flight-Flutter Test Program

Michael W. Kehoe

May 1984

NASA

National Aeronautics and
Space Administration

Highly Maneuverable Aircraft Technology (HiMAT) Flight-Flutter Test Program

Michael W. Kehoe
NASA Ames Research Center, Dryden Flight Research Facility, Edwards, California 93523

1984

NASA

National Aeronautics and
Space Administration
Ames Research Center
Dryden Flight Research Facility
Edwards, California 93523

SUMMARY

The highly maneuverable aircraft technology (HiMAT) vehicle was evaluated in a joint National Aeronautics and Space Administration and Air Force flight-test program. The HiMAT vehicle is a remotely piloted research vehicle. Its design incorporates the use of advanced composite materials in the wings, and canards for aeroelastic tailoring. A flight-flutter test program was conducted to clear a sufficient flight envelope to allow for performance, stability and control, and loads testing. Testing was accomplished with and without flight control-surface dampers. Flutter clearance of the vehicle indicated satisfactory damping and damping trends for the structural modes of the HiMAT vehicle. The data presented in this report include frequency and damping plotted as a function of Mach number.

SYMBOLS

ASE	aeroservoelastic	M_ℓ	limit Mach number
BCS	backup control system	PCS	primary control system
c	control surface chord length	V	true velocity
g	acceleration due to gravity	α	angle of attack, deg
$\bar{g}$	structural damping coefficient	ω	frequency, rad/sec
M	Mach number		

INTRODUCTION

The highly maneuverable aircraft technology (HiMAT) vehicle was built by Rockwell International for use in a joint National Aeronautics and Space Administration (NASA) and Air Force flight-test program. The vehicle was remotely piloted from a ground-based cockpit (ref. 1) and designed to demonstrate several advanced fighter technologies, including: (1) close-coupled canards that provide aerodynamic benefits, (2) active controls using a digital fly-by-wire system, (3) advanced composite and metallic structures, and (4) wing and canard aeroelastic tailoring.

The vehicle was launched from a B-52 aircraft at 13,716 m (45,000 ft) for each flight. The vehicle weight at launch (full fuel) was 1587 kg (3500 lb). The overall vehicle dimensions are presented in figure 1. The cruise or maneuver camber of the wing and canard supercritical airfoils could be selected between flights by changing leading edges. The difference in the leading edges is illustrated in figure 2.

A flutter-clearance program was conducted to verify the freedom from flutter within the flight envelope for the HiMAT vehicle. Clearance of the flutter envelope consisted of: flutter analysis (refs. 2 to 4), ground-vibration test (GVT) (ref. 5), wind-tunnel test (ref. 5), and flight-flutter test.

Rockwell International, North American Aircraft Operations, performed the flutter-analysis and wind-tunnel tests. The wind-tunnel testing was performed only for the

investigaton of shock-induced oscillations. The GVT which was supported by NASA and Rockwell International, was conducted by the Air Force Flight Test Center, Edwards AFB, California. Flight-flutter testing was conducted by the NASA Ames Dryden Flight Research Facility (DFRF) at Edwards, and supported by Rockwell International.

Test Objectives

The objectives of the program were to: (1) provide a flutter clearance for the HiMAT vehicle which would allow performance, stability and control, and loads testing to be accomplished, and (2) obtain frequency and damping information for critical structural modes of vibration.

Vehicle Description

Two HiMAT vehicles were constructed. The first vehicle (Ship 1, serial no. 870) served as the basis for envelope expansion which included supersonic flight. The second vehicle (Ship 2, serial no. 871) was used to probe the transonic region with emphasis on pressure and structural deflection measurements. Ship 2 was not origi- nally intended to be flown supersonically during the flight-test program.

After the subsonic flutter clearance, Ship 1 was equipped with elevator and ele- von control-surface dampers to prevent single-degree-of-freedom control surface flutter at supersonic speeds. These dampers were removed toward the end of the flight-test program. Ship 2 was not equipped with control-surface dampers since the vehicle was not intended to be flown at supersonic speeds. All flutter testing was conducted on Ship 1 (fig. 3).

Two independent digital flight-control systems have been implemented in the HiMAT vehicles. Each vehicle was flown in the primary control system (PCS) for normal research flight-test conditions. A backup control system (BCS) was provided to con- trol the vehicle in the event of certain airborne or ground failures which would pre- clude the use of the PCS (ref. 7). Transfer from the PCS to the BCS was designed to be automatic, but manual transfer could also be initiated.

The ailerons were mechanically locked out after the eighth flight, primarily as part of the new, relaxed, static stability-control system testing within the flight envelope. It should be noted that the ailerons were predicted to flutter at super- sonic speeds, and may have required dampers had they not been locked out. The rud- ders, elevons, elevators, and canard flaps were active for all flutter flights (fig. 1). The rudders were all movable surfaces, while all the other control sur- faces were hinged.

Instrumentation

Flutter instrumentation aboard Ship 1 consisted of the accelerometers and strain gages shown in figure 4. This instrumentation was used for all of the supersonic and some of the subsonic flutter testing. Instrumentation for the initial subsonic test- ing did not consist of the right-hand elevon and elevator accelerometers. However, an accelerometer was mounted on the forward and aft tip areas of the left canard and wing for the initial subsonic testing.

TEST APPROACHES AND PROCEDURES

Flight-Envelope Expansion

Flutter testing was accomplished at altitudes of 12,192 m (40,000 ft) and 7,620 m (25,000 ft). The maximum Mach numbers flown for data acquisiton were Mach 1.44 at 12,192 m (40,000 ft) and Mach 1.29 at 7,620 m (25,000 ft). Each flutter flight consisted of a constant-altitude, incremental Mach number flight-envelope expansion. The planned incremental test points are illustrated in figure 5. Angle-of-attack effects on damping were evaluated at selected transonic test conditions. The subsonic envelope was cleared, and then the supersonic envelope was cleared. Accomplishment of the 12,192-m (40,000-ft) test points always preceded accomplishment of the 7,620-m (25,000-ft) test points.

Excitation

The vehicle was excited at each test point by a sequence of control-surface pulses which were programmed into the ground-based computer. These pulses provided symmetric and antisymmetric excitation using the ailerons, canard flaps, elevons, and rudders. The aileron pulses were deleted from the sequence for the flights when the ailerons were mechanically locked on the vehicle. The execution time for the sequence of control-surface pulses was approximately 20 sec. The amplitude and duration of each control-surface pulse is illustrated in figure 6.

Random atmospheric turbulence was the primary source of excitation to the vehicle's structure. Typically, 1 min of data was collected at each subsonic test point, and 30 sec of data was acquired at each supersonic test point.

Envelope Expansion Procedure

A consistent procedure was used during the testing of the HiMAT vehicle. The pilot first stabilized the vehicle at the test altitude and specified Mach number. When the vehicle was stabilized, the structure was excited by control-surface pulses and random atmospheric turbulence.

Telemetered data were displayed on strip charts and were digitally stored on a disk in the DFRF spectral-analysis facility. Selected accelerometer responses were monitored on a real-time spectrascope to provide frequency-domain information. A Fourier analyzer was used for auto-power spectrum calculations to obtain frequency and damping information from the random data. The data were smoothed by multiplying the autocorrelation function by an exponential function. The half-power technique was used to estimate damping. The logarithmic decrement technique was employed to obtain frequency and damping information from the strip chart responses to control-surface pulses. Clearance to the next higher Mach number test point was given by the test director in the spectral-analysis facility after the damping coefficients and trends for the structural modes were observed to be satisfactory.

Postflight analysis performed between flights consisted of calculating the auto-power spectrum for each accelerometer response to extract the structural frequency and damping values.

TEST RESULTS

The aircraft-measured response to excitation was used to calculate frequency and damping values for each test point. As expected, the preprogrammed control-surface pulses could only excite the first symmetric bending modes for the canard and the wing. Random atmospheric turbulence was relied upon for excitation of the other higher-frequency structural modes. However, there was often insufficient atmospheric turbulence for good structural excitation because of the HiMAT high-altitude-only flight-test envelope. Therefore, it was difficult to consistently excite all structural modes of interest with an adequate signal-to-noise ratio. Analysis of modal data with a low signal-to-noise ratio results in scatter of the estimated damping values. However, random and control-surface pulse excitation were considered acceptable for this test program because (1) the flutter speed was predicted to be more than 20 percent greater than the planned maximum speed test point, (2) speed was increased by a small increment between test points, and (3) the HiMAT is a remotely piloted vehicle.

Subsonic data were acquired with both the cruise and maneuver leading edges installed on the vehicle. All supersonic test points were accomplished with the cruise leading edges only. The subsonic data results revealed no significant effects on the flutter characteristics of the vehicle because of the leading-edge configuration change.

The data also indicated that the installation of mechanical locks on the ailerons did not significantly affect the critical modal characteristics of the vehicle.

The effect of angle of attack on the modal damping was investigated. Turns at an elevated load factor and pushover-pullup maneuvers were performed in the transonic region to acquire the data. Analysis revealed that no definite trends could be established because of scatter in the data.

The plots of frequency and damping as a function of Mach number contain averaged data. These data were obtained for each mode by averaging the frequency and damping values calculated from several accelerometer responses. All frequency and damping data presented are from auto-power spectra analyses; these data are not presented for particular modes at some Mach numbers at which poor modal excitation was experienced. Atmospheric turbulence sometimes failed to adequately excite a mode with a low energy content, resulting in a low reliability of the calculated damping value because the random excitation was of almost the same magnitude as was the magnitude of the noise. The plots displayed were faired with least-squared error lines so that general data trends could be followed. The structural modes were identified with names based on data in reference 5.

Test Data at 12,192 m (40,000 ft)

The frequency and damping trends at 12,192 m (40,000 ft) are presented in figures 7 to 12. No adverse damping trends were exhibited for the modes that were tracked. The maximum Mach number at which data were obtained was Mach 1.44.

The damping trend for the symmetric canard bending mode (fig. 9) exhibited a decrease in damping in the transonic region; however, the level of damping increased in the supersonic region.

4

Test Data at 7,620 m (25,000 ft)

The frequency and damping trends at 7,620 m (25,000 ft) are presented in figures 13 to 18. The damping trends and levels were satisfactory from a flutter standpoint. The maximum Mach number at which data were obtained was Mach 1.29.

The flight-test envelope presently cleared for the HiMAT vehicle is illustrated in figure 19. The envelope limits were established by the maximum Mach number (1.44) and the maximum equivalent airspeed (518 KEAS) at which data were acquired. This envelope is less than the HiMAT maximum design capability. More flight-flutter testing would be required if further envelope expansion were desired.

Control Surface Free Play

The first three flights of the vehicle were flown with excessive free play in the control surfaces. Flutter testing on the second and third flights revealed lightly damped oscillations on the canard and wing.

Extrapolation of the damping trend for the canard indicated possible flutter at Mach 0.95 at 12,192 m (40,000 ft). Frequency and damping trends of the wing and canard were obtained after flights 2 and 3 by autocorrelation/direct Fourier transform analyses performed by Rockwell International (ref. 8). Subsequent to flight 3, a flutter analysis (ref. 8) with free play included was accomplished. The results of the analysis are presented in figure 20. The boundary correlates closely with the flight-test damping trends from flights 2 and 3.

The free play of all the control surfaces was significantly reduced by modifying the control-surface actuator bolts. Limits were specified (ref. 9) for each control surface (table 1), and the free play was measured after each flight to ensure that these limits were not exceeded. Flutter testing was conducted on flight 4, and a significant improvement in damping was noted. Figure 21 shows a comparison of damping trends and levels with and without free play. The damping estimates shown in figure 21 were obtained from control-surface pulses using the logarithmic decrement method (ref. 8). Note that the damping estimates exhibited in figures 13 (symmetric wing bending) and 15 (symmetric canard bending) are slightly different than the values shown in figure 21. The differences are likely due to the different techniques (logarithmic decrement and auto-power spectrum) of analysis.

Aeroservoelasticity

During flight testing, the HiMAT vehicle was monitored for possible aeroservoelastic (ASE) instabilities. Such instabilities occur when the flight-control system dynamically interacts with structural modes. Adverse structural coupling of the flight-control system was observed with the first symmetric wing-bending mode (9 Hz) on two occasions. This coupling occurred in the pitch axis when BCS was engaged at Mach 0.88 at 11,278 m (37,000 ft), and at Mach 0.91 at 12,802 m (42,000 ft). No adverse coupling was noted while the vehicle was operated in the primary flight-control system.

Time history traces of the BCS coupling with the 9-Hz structural mode at Mach 0.88 at 11,278 m (37,000 ft) are presented in figure 22. Note that the wing oscillations are limited in amplitude. During the BCS engagement at Mach 0.91 at

5

12,802 m (42,000 ft), the vehicle was decelerated from Mach 0.91 to Mach 0.80.
The 9-Hz oscillations remained constant in amplitude throughout the deceleration.

Several other transfers to the BCS occurred at altitudes below 11,278 m
(37,000 ft). No structural coupling was observed in the BCS. The maximum dynamic
pressure at which the BCS was engaged was 3.83 N/cm^2 (800 psf) at Mach 1.2 and
7,620 m (25,000 ft).

Control-Surface Dampers

Control-surface-rotation frequency measurements indicated that the control sur-
faces on the HiMAT vehicle had insufficient restraint stiffness to meet Rockwell's
single-degree-of-freedom flutter (buzz) criterion and could therefore be susceptible
to buzz instabilities. This buzz criterion was established from a Rockwell study and
is summarized in figure 23. The criterion does not include the effects of structural
damping, angle of attack, and airfoil shape. The study indicated that buzz would not
occur below a reduced velocity (V/cω) of 1.5, regardless of Mach number. The study
also indicated that the most critical Mach number was approximately 1.25. Note that
the unstable flight-test points are in the Mach number range of 1.0 to 1.1. It may
be inferred from this study that the higher the reduced velocity is above 1.5, the
more likely that the control surface is to buzz.

Using this criterion, frequency-versus-reduced-velocity curves were generated
for the control surfaces on both HiMAT vehicles (fig. 24). The rudders were all-
movable surfaces. Therefore, the buzz criterion does not apply to the rudders on the
HiMAT vehicle. When the measured control-surface-rotation frequency values for both
of the HiMAT vehicles were plotted on figure 24, the magnitude of the frequency defi-
cit was clearly indicated. As a result, detailed supersonic control-surface flutter
analyses were required to establish mechanical damper requirements. The analyses
assumed no structural damping in the determination of the control-surface viscous
dampers, primarily because of the unreliable nature of actuator system damping.
These analyses predicted that the existing hinge-line rotational stiffness was suf-
ficient to prevent canard flap, single-degree-of-freedom flutter, but that the ele-
vons and elevators would require dampers.

Elevon and elevator dampers were installed on Ship 1. The vehicle was flown to
Mach 1.44 at 12,192 m (40,000 ft) with no indications of control-surface buzz at any
Mach number.

It became desirable to fly Ship 2 supersonically so that wing and canard pressure
distribution and deflection measurement data could be gathered. Ship 2 was not
equipped with control-surface dampers. Because of money and time constraints, it was
decided not to modify Ship 2 with dampers, but to clear Ship 1 to fly supersonically
with the control-surface dampers removed, thus clearing Ship 2 so that it could fly
without control-surface dampers. Ship 1 was flown without dampers to Mach 1.2 at
12,192 m (40,000 ft) and to Mach 1.29 at 7,620 m (25,000 ft) with no indications of
buzz. Ship 2 was flown without dampers to Mach 1.2 at 12,192 m (40,000 ft), Mach 1.25
at 11,582 m (38,000 ft) and Mach 1.2 at 7,620 m (25,000 ft) with no indications of
buzz.

The buzz criterion and the results of the single-degree-of-freedom control-surface
flutter analyses proved to be conservative when compared with the flight results of
the HiMAT with the dampers removed. The lack of agreement between the buzz criterion
and the flight-test results may be a result of the inability of the criterion to

account for the effects of structural damping, airfoil shape, and angle of attack. The lack of correlation between the analyses and flight-test results may be due to the inaccuracies of the analytical representation of the unsteady aerodynamics. Another possible explanation is that the assumption of no structural damping in the analysis was conservative. The rationale for this assumption is that as flight time increases on a vehicle, the wear and tear on the control-system actuators can cause a significant reduction in the inherent structural damping. However, for the HiMAT vehicle, the regular maintenance of the control system and the postflight free-play checks would have prevented any significant reduction in the actuator-system damping.

CONCLUSIONS

A flight-flutter test program was successfully completed for the HiMAT vehicle. Data were acquired at Mach 1.44 and Mach 1.29 at 12,192 m (40,000 ft) and 7,620 m (25,000 ft), respectively. The damping levels and trends were satisfactory from a flutter standpoint. Three flights were flown with an excessive amount of free play in the control surfaces. Lightly damped oscillations were recorded for the wing and canard on the second and third flights. Extrapolation of the damping trends revealed a possibility of flutter at Mach 0.95 at 12,192 m (40,000 ft). Subsequent to the third flight, the free play was removed, and a significant improvement in damping was exhibited on the fourth flight.

HiMAT Ship 1 was flown to supersonic speeds with and without dampers on the elevon and elevator control surfaces. Single-degree-of-freedom control-surface flutter was not experienced for either configuration, although the buzz criterion and analyses indicated that the damper-off configuration was susceptible to flutter.

A coupling of the flight-control system with first symmetric wing-bending mode (9 Hz) was experienced at an altitude of 11,278 m (37,000 ft) and above while in the BCS. The resulting oscillation was limited in amplitude. The BCS did not exhibit this instability below 11,278 m (37,000 ft).

Ames Research Center
  Dryden Flight Research Facility
    National Aeronautics and Space Administration
      Edwards, California, March 9, 1983

7

REFERENCES

1. Arnaiz, H. H.; and Loschke, P. C.: Current Overview of the Joint NASA/USAF HiMAT Program. NASA CP-2162, Part 1, 1981, pp. 91-121.

2. Siegel, S.: HiMAT Post-GVT Flutter Analysis. NA-79-366, Rockwell International, North American Aircraft Div., Los Angeles, Calif., Aug. 7, 1979.

3. Siegel, S.: HiMAT Flutter Analysis. NA-78-708, Rockwell International, North American Aircraft Div., Los Angeles, Calif. Sept. 11, 1978.

4. Siegel, S.: Preliminary Flutter Analysis of the HiMAT/RPRV Air Vehicle. DAR11420-01, Rockwell International, North American Aircraft Div., Los Angeles, Calif., Apr. 15, 1976.

5. Coombs, David F.: Ground Vibration Test of the Highly Maneuverable Aircraft Technology (HiMAT) Vehicle. AFFTC-TR-78-31, Air Force Flight Test Center, Edwards, Calif., Mar. 1979.

6. Stevenson, J. R., Shock-Induced Self-Excited Airfoil Bending Oscillations. NA-78-723, Rockwell International, North American Aircraft Div., Los Angeles, Calif., Oct. 1978.

7. Myers, Albert F.; Earls, Michael R.; and Callizo, Larry A.: HiMAT Onboard Flight Computer System Architecture and Qualifications. AIAA Paper 81-2107, Oct. 1981.

8. Dobbs, S. K., and Siegel, S.: HiMAT Flutter Characteristics with Control Surface Free Play: Flight Test and Analysis. TFD-80-394, Rockwell International, North American Aircraft Div., Los Angeles, Calif., Aug. 1, 1980.

9. Military Specification: Airplane Strength and Rigidity — Flutter, Divergence and Other Aeroelastic Instabilities. MIL-A-008870A (USAF), Mar. 31, 1971.

TABLE 1. - CONTROL SURFACE FREE-PLAY LIMITS

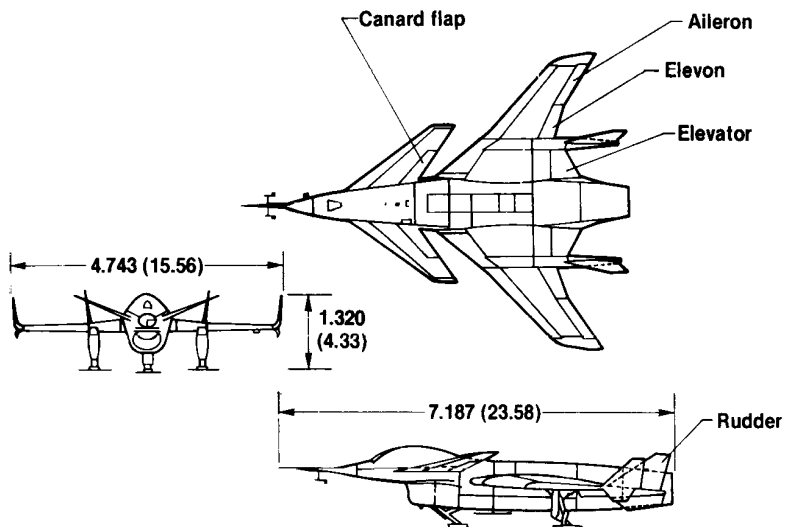| Control surface	Free-play limit, deg
Aileron	0.13
Elevon	0.286
Elevator	0.286
Rudder	0.034
Canard flap	0.13

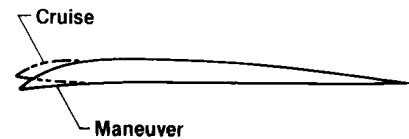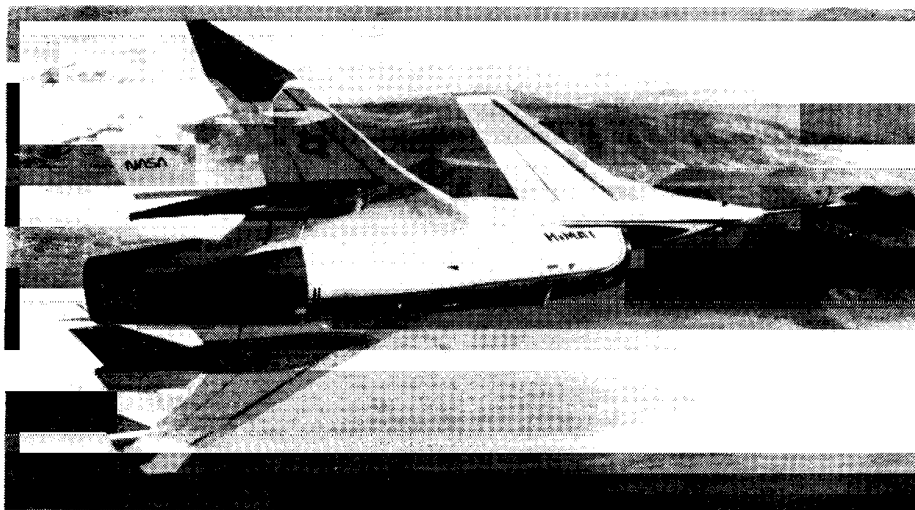Figure 1. HiMAT vehicle. Dimensions in meters (feet).

Figure 2. Cruise and maneuver camber leading edge for wing and canard airfoil section (interchangeable between flights).

ECN 14281

Figure 3. HiMAT test vehicle in flight.

9

1. Right canard
2. Right canard flap
3. Left canard flap
4. Left canard
5. Right wingtip
6. Right elevon
7. Right elevator
8. Left elevator
9. Left elevon
10. Left wingtip
11. Left winglet
12. Left rudder
13. Right rudder

▲ Normal accelerometer
● Hinge-moment strain gage
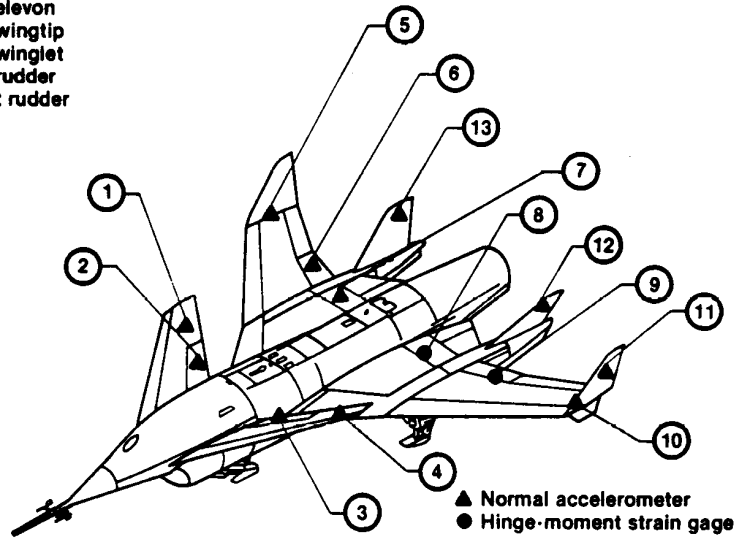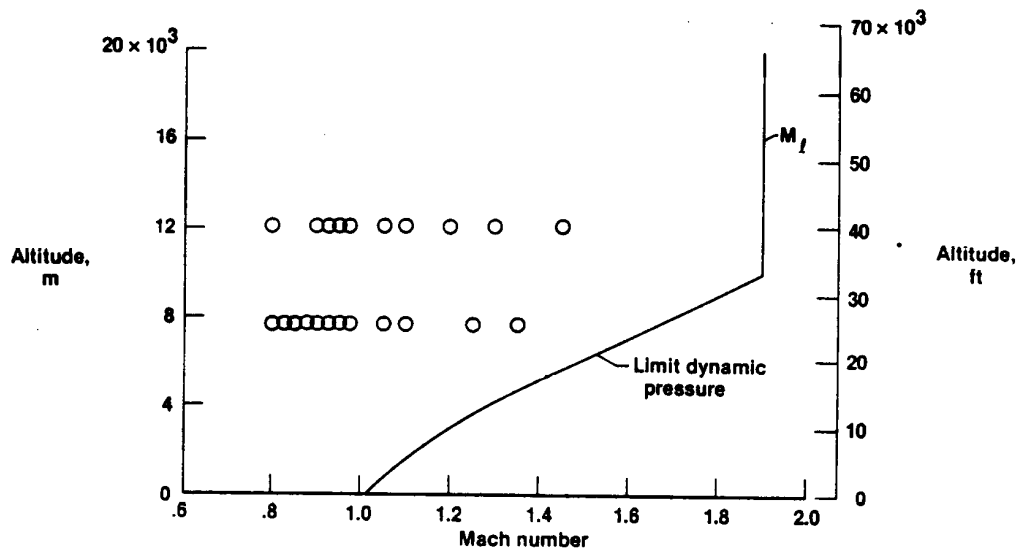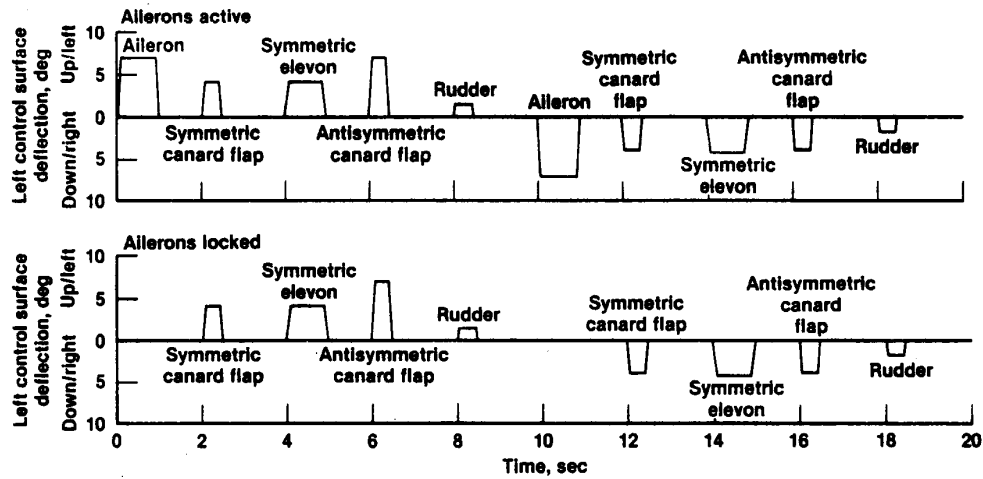
Figure 4. Vehicle instrumentation location.

Figure 5. Planned flight-test points.

Figure 6. *Automatic flight control pulse sequence. Right control surface deflections were equal in magnitude to the left surface deflections; the direction of the right surface deflections corresponds to the symmetry noted for each pulse.*
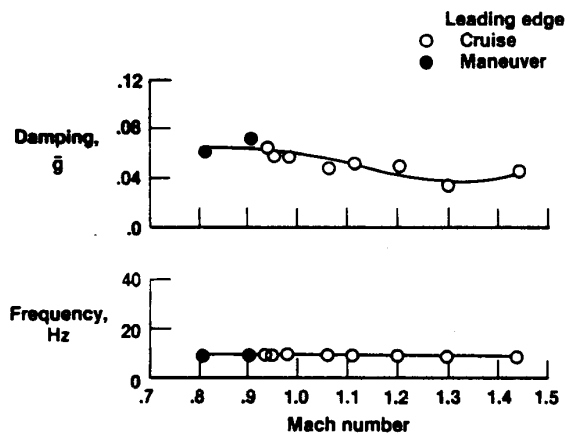

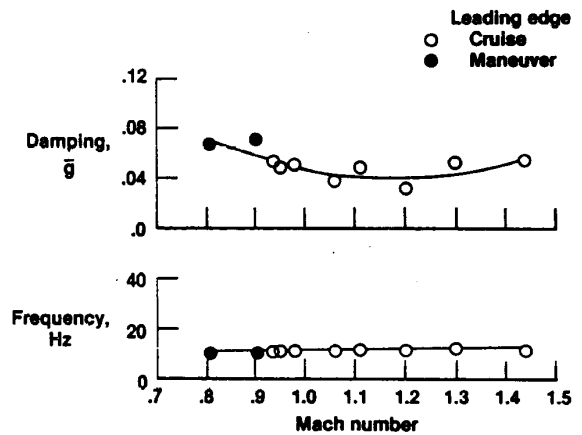Figure 7. *Symmetric wing-bending modal data. Altitude = 12,192 m (40,000 ft).*

Figure 8. *Antisymmetric wing-bending modal data. Altitude = 12,192 m (40,000 ft).*
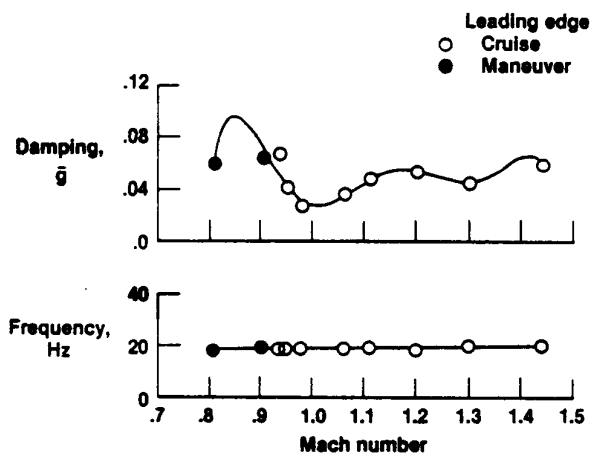
11

Figure 9. Symmetric canard-bending modal data. Altitude = 12,192 m (40,000 ft).
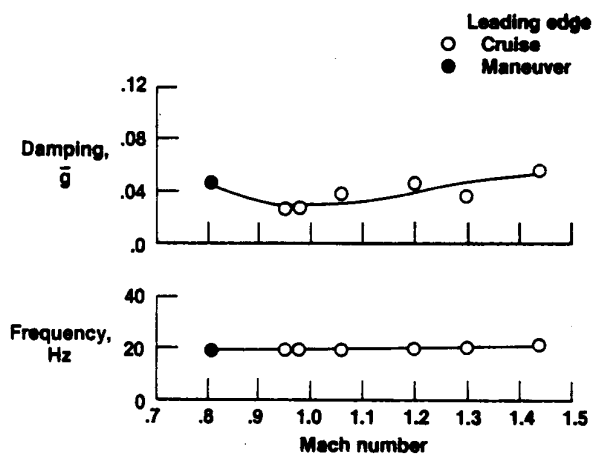

Figure 10. Antisymmetric canard-bending modal data. Altitude = 12,192 m (40,000 ft).
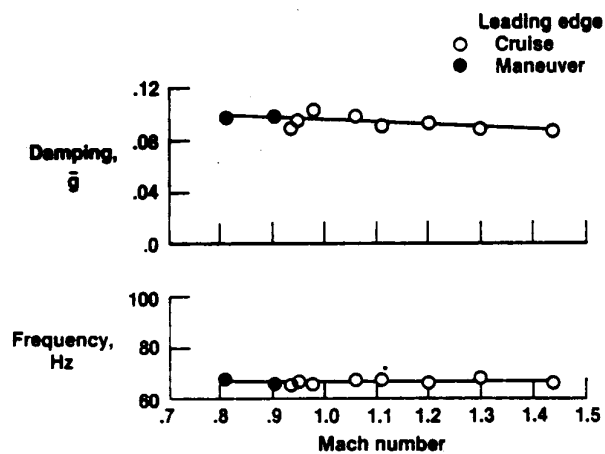

Figure 11. Canard torsion modal data. Altitude = 12,192 m (40,000 ft).

Figure 12. Winglet-bending modal data. Altitude = 12,192 m (40,000 ft).

Figure 13. *Symmetric wing-bending modal data.* *Altitude = 7620 m (25,000 ft).*
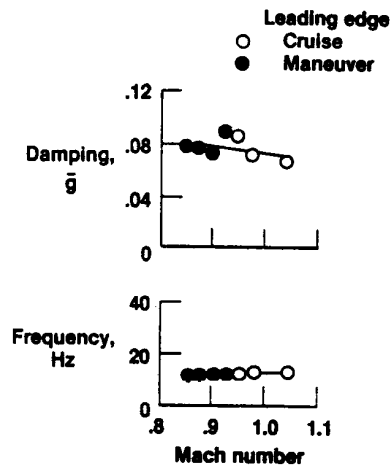
Figure 14. *Antisymmetric wing-bending modal data.* *Altitude = 7620 m (25,000 ft).*
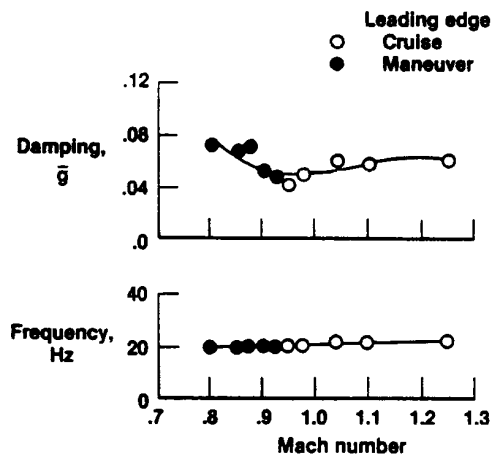
Figure 15. *Symmetric canard-bending modal data.* *Altitude = 7620 m (25,000 ft).*
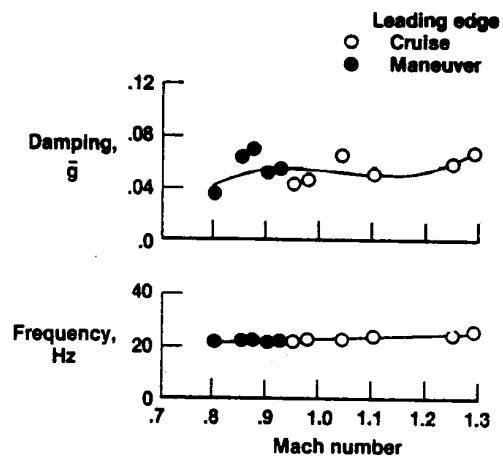
Figure 16. *Antisymmetric canard-bending modal data.* *Altitude = 7620 m (25,000 ft).*

13

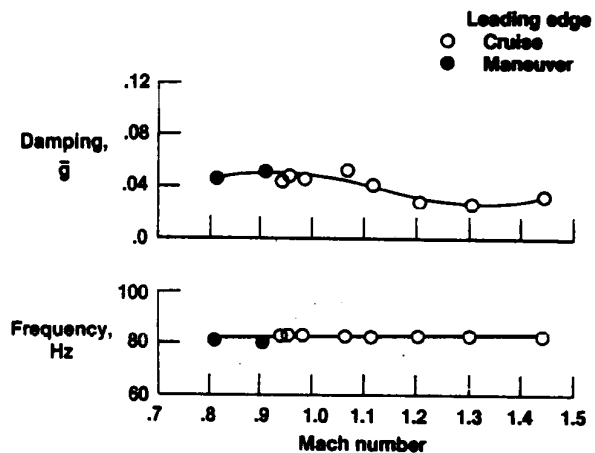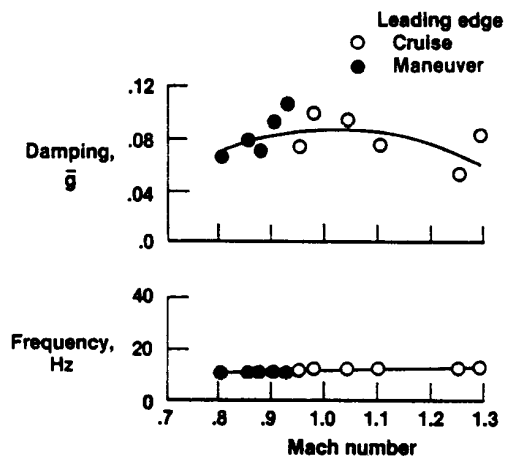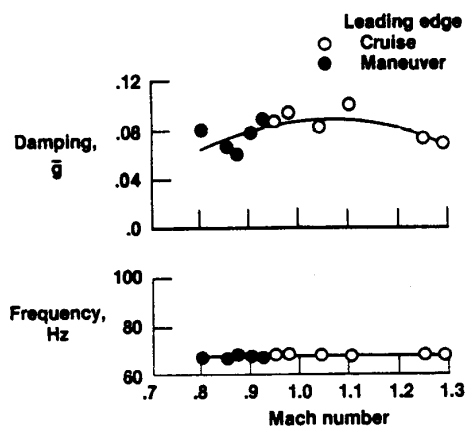Figure 17. *Canard torsion modal data. Altitude = 7620 m (25,000 ft).*
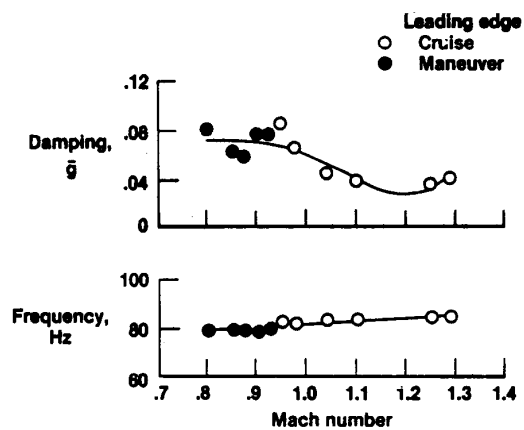
Figure 18. *Winglet-bending modal data. Altitude = 7620 m (25,000 ft).*
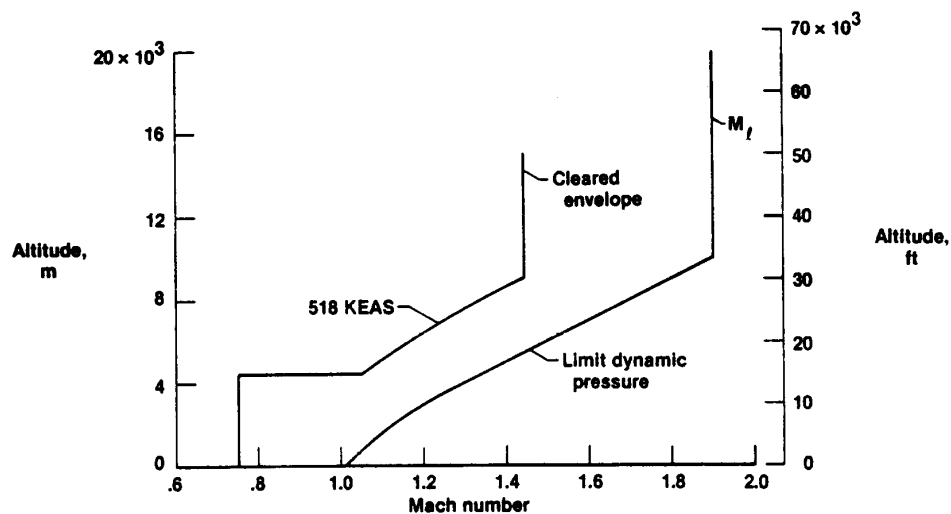
Figure 19. *Cleared flutter envelope.*

14
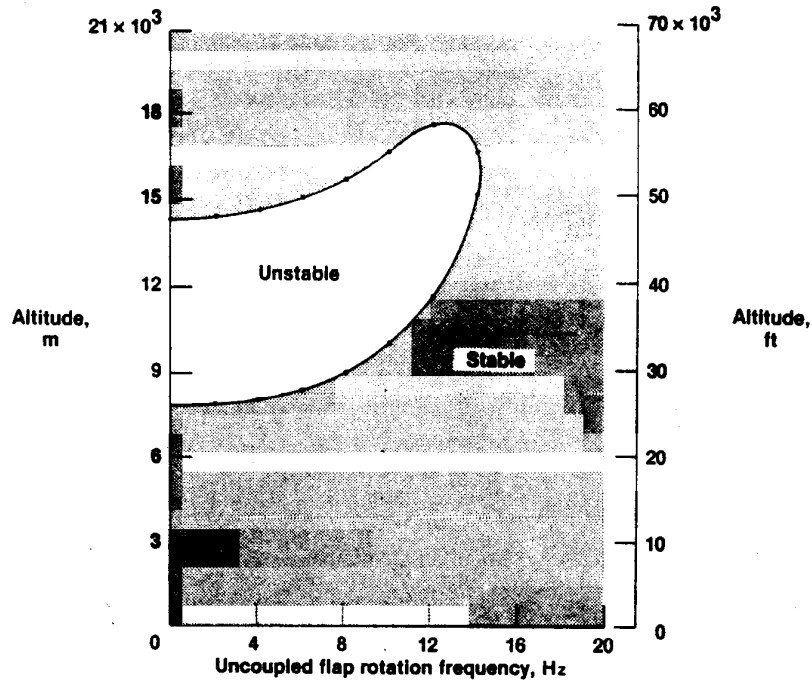
Figure 20. Canard flutter-analysis results. Canard first bending and flap rotation; M = 0.95; match point solutions at $\bar{g}$ = 0.
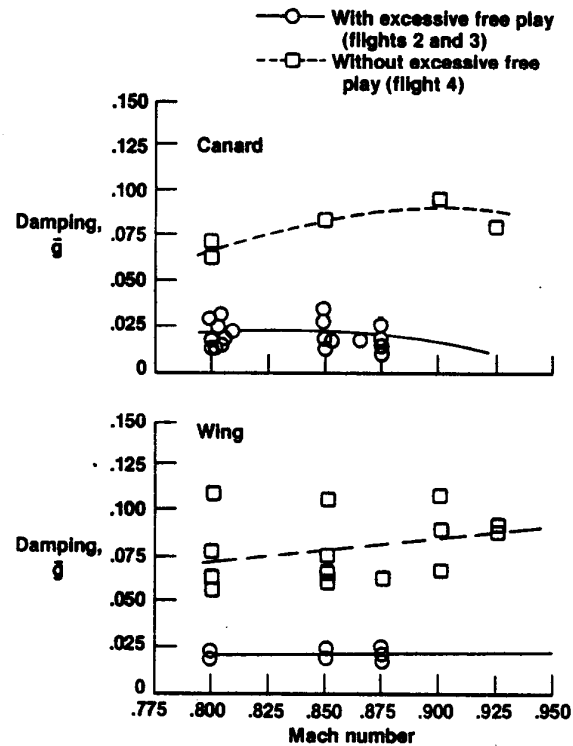
Figure 21. Symmetric wing- and canard-bending modal data comparison. Altitude = 7620 m (25,000 ft).
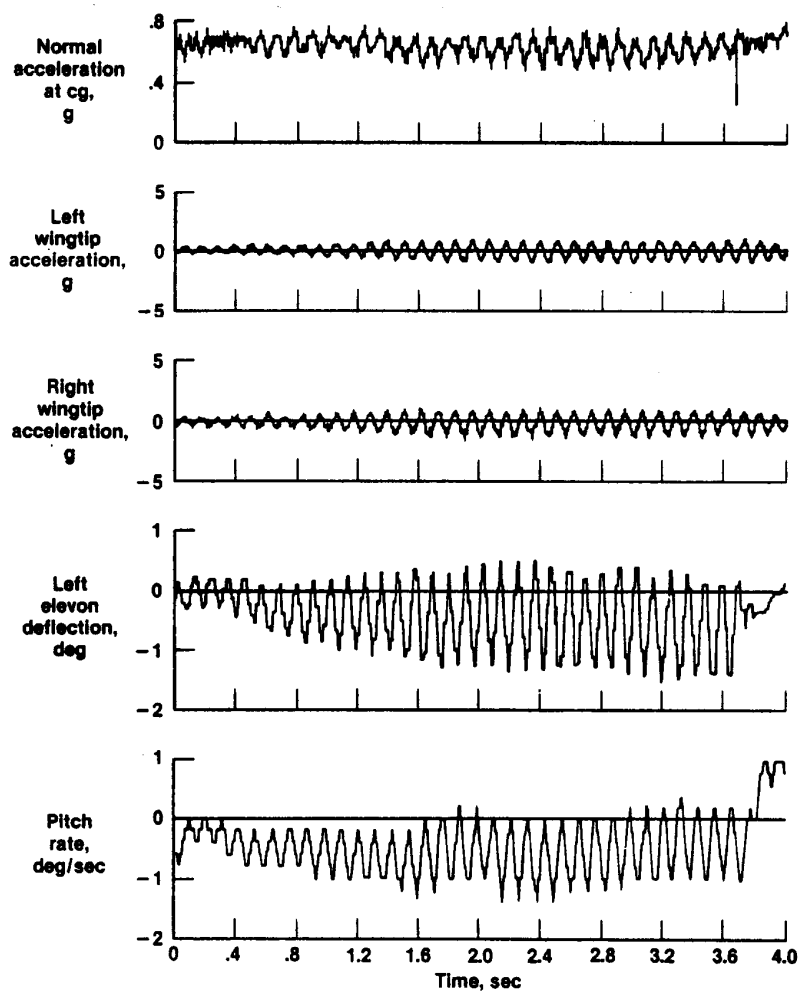
Figure 22. Time history of wing oscillation. BCS flight control mode; M = 0.88; altitude = 11,278 m (37,000 ft).

Flutter

Reduced
velocity,
V/cω

No flutter

Mach number
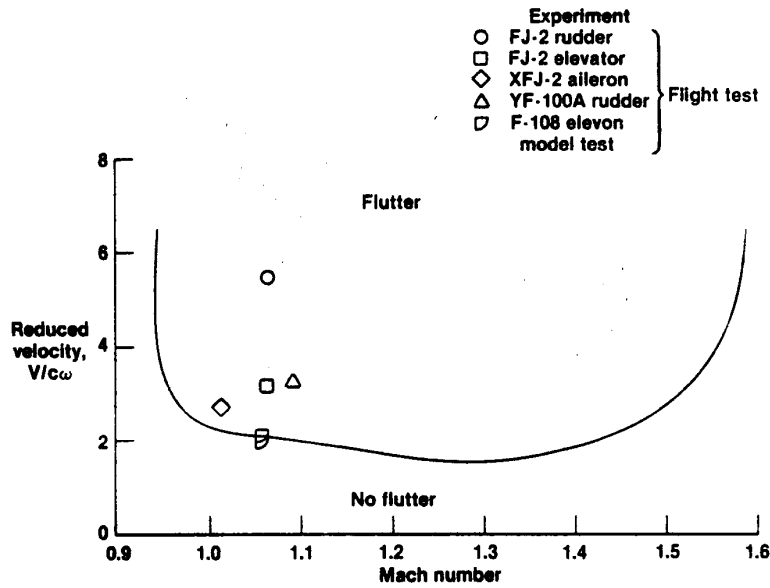
Figure 23. *Control-surface flutter criterion.*

□ Ship 1
O Ship 2

Frequency,
Hz

Elevator

Elevon and canard flap

Aileron

Canard flap

Elevon

V/cω

Figure 24. *HiMAT buzz requirements.*
M = 1.25; altitude = 12,192 m
(40,000 ft).

1. Report No. NASA TM-84907	2. Government Accession No.	3. Recipient's Catalog No.
4. Title and Subtitle Highly Maneuverable Aircraft Technology (HiMAT) Flight-Flutter Test Program		5. Report Date May 1984
		6. Performing Organization Code
7. Author(s) Michael W. Kehoe		8. Performing Organization Report No. H-1183
9. Performing Organization Name and Address NASA Ames Research Center Dryden Flight Research Facility P.O. Box 273 Edwards, California		10. Work Unit No.
		11. Contract or Grant No.
12. Sponsoring Agency Name and Address National Aeronautics and Space Administration Washington, D.C. 20546		13. Type of Report and Period Covered Technical Memorandum
		14. Sponsoring Agency Code RTOP 533-03-11

15. Supplementary Notes

16. Abstract

The highly maneuverable aircraft technology (HiMAT) vehicle was evaluated in a joint National Aeronautics and Space Administration and Air Force flight-test program. The HiMAT vehicle is a remotely piloted research vehicle. Its design incorporates the use of advanced composite materials in the wings, and canards for aeroelastic tailoring. 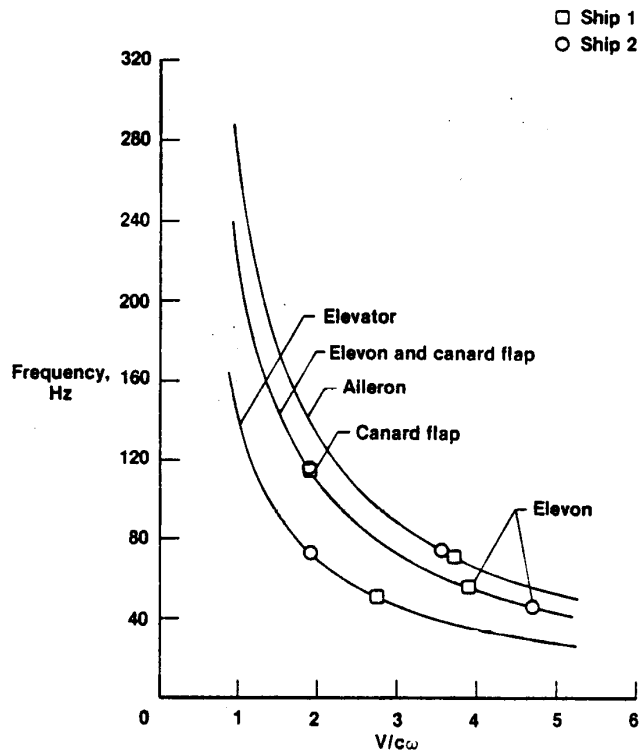A flight-flutter test program was conducted to clear a sufficient flight envelope to allow for performance, stability and control, and loads testing. Testing was accomplished with and without flight control-surface dampers. Flutter clearance of the vehicle indicated satisfactory damping and damping trends for the structural modes of the HiMAT vehicle. The data presented in this report include frequency and damping plotted as a function of Mach number.

17. Key Words (Suggested by Author(s)) Remotely piloted vehicle Flight flutter Control surface buzz Control surface free play Aeroservoelasticity	18. Distribution Statement FEDD distribution STAR category 05

19. Security Classif. (of this report) Unclassified	20. Security Classif. (of this page) Unclassified	21. No. of Pages 18	22. Price* A02

*Available through NASA's Industrial Application Centers.